Proc. Natl. Acad. Sci. USA
Vol. 87, pp. 7893–7897, October 1990
Biophysics

Steady-state force–velocity relation in the ATP-dependent sliding movement of myosin-coated beads on actin cables *in vitro* studied with a centrifuge microscope

(actin–myosin interaction/force–velocity relation/muscle contraction)

KAZUHIRO OIWA*, SHIGERU CHAEN*, EIJI KAMITSUBO†, TERUO SHIMMEN‡, AND HARUO SUGI*

*Department of Physiology, School of Medicine, Teikyo University, Itabashi-ku, Tokyo 173, Japan; †Biological Laboratory, Hitotsubashi University, Kunitachi, Tokyo 186, Japan; and ‡Department of Botany, Faculty of Science, University of Tokyo, Bunkyo-ku, Tokyo 113, Japan

Communicated by William F. Harrington, July 19, 1990 (received for review May 15, 1990)

ABSTRACT **To eliminate the gap between the biochemistry of actomyosin in solution and the physiology of contracting muscle, we developed an *in vitro* force–movement assay system in which the steady-state force–velocity relation in the actin–myosin interaction can be studied. The assay system consists of the internodal cells of an alga, *Nitellopsis obtusa*, containing well-organized actin filament arrays (actin cables); tosyl-activated polystyrene beads (diameter, 2.8 μm; specific gravity, 1.3) coated with skeletal muscle myosin; and a centrifuge microscope equipped with a stroboscopic light source and a video system. The internodal cell preparation was mounted on the rotor of the centrifuge microscope, so that centrifugal forces were applied to the myosin-coated beads moving along the actin cables in the presence of ATP. Under constant centrifugal forces directed opposite to the bead movement ("positive" loads), the beads continued to move with constant velocities, which decreased with increasing centrifugal forces. The steady-state force–velocity curve thus obtained was analogous to the double-hyperbolic force–velocity curve of single muscle fibers. The unloaded velocity of bead movement was 1.6–3.6 μm/s (20–23°C), while the maximum "isometric" force generated by the myosin molecules on the bead was 1.9–39 pN. If, on the other hand, the beads were subjected to constant centrifugal forces in the direction of bead movement ("negative" loads), the bead also moved with constant velocities. Unexpectedly, the velocity of bead movement did not increase with increasing negative loads but first decreased by 20–60% and then increased towards the initial unloaded velocity until the beads were eventually detached from the actin cables.**

Although the recent development of *in vitro* assay systems for the ATP-dependent actin–myosin interaction has made it possible to study the sliding movement between actin and myosin (1–4), a large gap still exists between the biochemistry of the actomyosin system in solution and the physiology of contracting muscle, as in these systems the actin–myosin sliding takes place only under unloaded conditions. In an attempt to eliminate the above gap, we have developed an *in vitro* assay system in which a myosin-coated glass needle of a known elastic coefficient slides along the well-organized arrays of actin filaments (actin cables) in the internodal cell of an alga *Nitellopsis* in the presence of ATP, so that both the force and the sliding movement caused by the ATP-dependent actin–myosin interaction can be recorded simultaneously (5). With this force–movement assay system, we have obtained a convex-shaped force–velocity (*P–V*) relation analogous to that of single muscle fibers in the auxotonic condition (6); however, in this force–movement assay system, it was not possible to maintain constant forces.

The publication costs of this article were defrayed in part by page charge payment. This article must therefore be hereby marked "*advertisement*" in accordance with 18 U.S.C. §1734 solely to indicate this fact.

Since a most basic characteristic of contracting muscle is that it shortens with a constant velocity while generating a constant force equal to the external load, thus giving rise to a hyperbolic *P–V* relation (7), we have further constructed another force–movement assay system with which the steady-state *P–V* relation of the ATP-dependent actin–myosin interaction can be studied. The assay system consists of the internodal cell of *Nitellopsis* containing the actin cables, tosyl-activated polystyrene beads coated with skeletal muscle myosin, and a centrifuge microscope equipped with a stroboscopic light source and a video system. The internodal cell preparation was mounted on the rotor of the centrifuge microscope to apply constant centrifugal forces to the myosin-coated beads moving on the actin cables in the preparation in the presence of ATP. It will be shown that, under centrifugal forces directed opposite to the bead movement ("positive load"), the beads continued to move with constant velocities, and the steady-state *P–V* relation obtained was analogous to the double hyperbolic *P–V* relation in single muscle fibers (8), indicating that this assay system retains the basic characteristic of contracting muscle. Moreover, an unexpected finding brought about in the present study was that, under centrifugal forces in the direction of bead movement ("negative loads"), the velocity of bead movement did not increase but decreased below the initial unloaded velocity. These results indicate that the present force–movement assay system is useful not only for connecting muscle biochemistry with muscle physiology but also for revealing the unexpected features of the actin–myosin interaction.

MATERIAL AND METHODS

Preparation of the Myosin-Coated Polystyrene Beads. Myosin was prepared from rabbit skeletal muscle (9) and stored in 50% (vol/vol) glycerol/0.3 M KCl/0.2 mM $NaHCO_3$/1 mM dithiothreitol at −20°C. Before use, stored myosin was washed twice with 0.5 M KCl/20 mM Pipes, pH 7.0/1 mM dithiothreitol to prepare a myosin sample at a concentration of 1 mg/ml in 50 mM KCl/20 mM Pipes, pH 7.0/0.1 mM dithiothreitol.

Tosyl-activated polystyrene beads (Dynabeads; Dynal, Oslo; diameter, 2.8 μm; specific gravity, 1.3) were incubated with the myosin sample (10^7 beads per ml) in 50 mM sodium carbonate/bicarbonate (pH 9.0) for 60 min at 0°C. The solution was then diluted 1:9 with 20 mM Pipes (pH 7.0), and the myosin-coated beads were precipitated by centrifugation and resuspended in Mg·ATP solution containing 5 mM EGTA, 6 mM $MgCl_2$, 1 mM ATP, 200 mM sorbitol, 50 mM KOH, and 20 mM Pipes (pH 7.0).

Internodal Cell Preparation. The green alga *Nitellopsis obtusa* was cultured by the method of Shimmen and Yano (2). Before the experiments, the internodal cells (diameter,

≈0.5mm; length, 12–17cm) were isolated from neighboring cells and stored in artificial pond water containing 0.1 mM each KCl, NaCl, and $CaCl_2$ (pH ≈ 5.6). The internodal cell preparation was prepared in the following way. The cell was cut open at both ends, and the cell sap was replaced with Mg·ATP solution by perfusing the cell interior with the solution several times the cell volume (2, 10). At the late stage of the perfusion, the myosin-coated polystyrene beads were introduced into the cell. After the perfusion, both ends of the cell containing the myosin-coated beads were ligated with strips of polyester thread (see Fig. 1). The internodal cell preparations (length, ≈1 cm) were kept in artificial pond water.

Centrifuge Microscope and Video System. The centrifuge microscope was composed of a light microscope, a rotor (diameter, 16 cm) that can be rotated at 250–5000 rpm (4–1900 × *g*), and a stroboscopic light source (Fig. 1*A*). The rotor had a groove to which an Acrylite centrifuge cuvette (33 × 20 × 3 mm deep, Fig. 1*B*) was mounted, its rate of rotation being controlled by changing the supply voltage to the motor. The effective radius for centrifugation of the specimen could be adjusted in the range of 45–70 mm. The light source was a xenon tube that was triggered repetitively to generate light flashes (duration, ≈180 ns). To trigger the xenon tube each time, the specimen in the cuvette came under the objective lens, the position of a metal piece at the rotor edge opposite to the cuvette was sensed by a light source–photodiode device, and the light signal was converted into an electrical pulse to trigger the xenon tube. Thus, the stationary image of the specimen could be observed during the course of centrifugation of the specimen. The electrical pulse was also fed to a pulse-counter circuit to monitor the rate of rotation of the rotor. The speed of the rotor in rpm was displayed digitally (with an accuracy of three figures) on the video monitor screen.

The video-enhanced contrast image of the specimen was obtained with a video-camera (C-2847, Hamamatsu Photonics, Hamamatsu, Japan) combined with the circuits for real-time differential treatment of the image signal (Fig. 2).

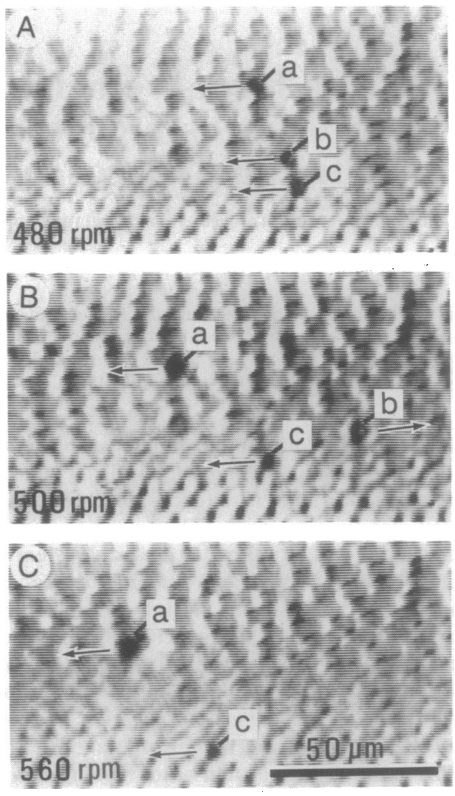

FIG. 2. Selected video frames showing the myosin-coated beads moving on the actin cables under three different rotation rates of the rotor indicated in each frame. Arrows show the direction of the bead movement. (*A*) Beads a, b, and c move forward with nearly the same velocities. (*B*) Beads a and c continue to move forward, while bead b just starts to go backward because the amount of positive load by the applied centrifugal force exceeds P_o of bead b. (*C*) Beads a and c still move forward.

The video image was observed on the monitor screen and recorded with a video cassette recorder (VO-9600, Sony) at

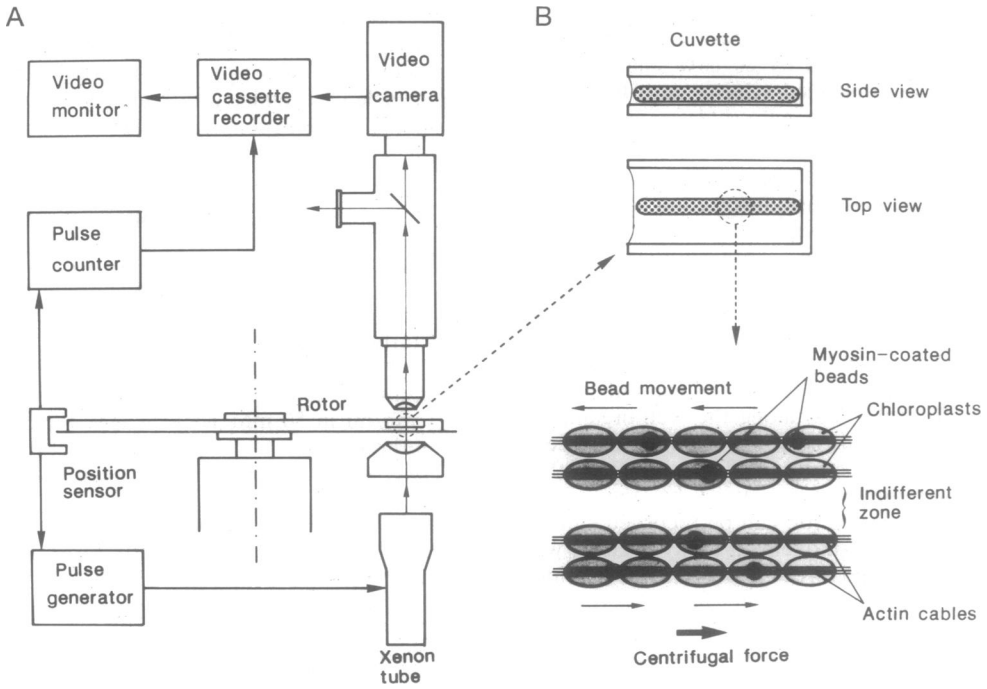

FIG. 1. Diagram of the experimental arrangement. (*A*) Composition of the centrifuge microscope and the video system. (*B*) Principle of application of centrifugal forces serving as positive or negative loads to the myosin-coated beads moving on the actin cables. Note that the direction of the bead movement is reversed across the indifferent zone. For further explanation, see text.

30 frames per s. Further details of the centrifuge microscope and the video system have been described elsewhere (11).

Experimental Procedures. The internodal cell preparation containing the myosin-coated beads was put into the cuvette filled with artificial pond water in such a way that its chloroplast rows, along which the actin cables extended straight, were parallel to the direction of centrifugal force (Fig. 1*B*). The unidirectional bead movement along the actin cables was observed with a Nikon ×40 dry objective (n.a., 0.55). Attention was only focused on the beads that moved smoothly over many seconds not only under the unloaded condition but also under various rates of rotation of the rotor. All experiments were performed at 20–23°C.

The amount of centrifugal force (= load) F on the bead is given by:

$$F = \Delta\rho V r\omega^2,$$

where $\Delta\rho$ is the difference in density between the bead and the surrounding medium, V is the bead volume, r is the effective radius of centrifugation, and ω is the angular velocity of the rotor. In the present study, the values of $\Delta\rho$ and V were 0.3 and 12 μm^3, respectively. The bead movement under constant centrifugal forces was analyzed on replay from the video cassette recorder, the changes in the position of the bead being measured from frame to frame on the monitor screen with an accuracy of <0.5 μm (30 × 20 cm; magnification, ×2000) by a video microscaler (Fig. 1*A*).

RESULTS

Nature of the Response of the Myosin-Coated Beads to Centrifugal Forces Directed Opposite to the Bead Movement. Fig. 2 contains selected video frames showing the myosin-coated beads moving along the actin cables in one direction determined by the polarity of the actin filaments (1, 2). In many cases, more than two beads were observed in a microscopic field to move smoothly with nearly the same velocities under the unloaded condition. When centrifugal forces directed opposite to the bead movement were applied to serve as positive loads on the beads (Fig. 1*B*), the resulting decrease in the velocity of bead movement was not uniform but differed from bead to bead; under a given centrifugal force, some beads were detached from the actin cables to move away in the direction of centrifugal force, while the other beads still continued moving. These observations indicate that a considerable variation in the load-bearing ability exists among the beads, even though their unloaded velocity of movement is nearly the same.

Fig. 3 shows a typical effect of various centrifugal forces serving as positive loads on the movement of a bead that showed smooth movement over a wide range of applied forces. It was found that, under a constant centrifugal force, the bead moved with a constant velocity over many seconds, indicating the presence of a definite steady-state relation between the force (= load) generated by the actin–myosin interaction and the velocity of the actin–myosin sliding. When the load on the bead eventually reached a value equal to the maximum isometric force (P_o) generated by the myosin molecules on the bead, the bead stopped moving to stay at the same position for 5–10 s and was suddenly detached from the actin cable to flow away in the direction of centrifugal force.

The values of P_o measured in the present study showed a considerable variation, ranging from 1.9 to 39 pN (mean, 19 pN; n = 18). If the maximum force exerted by each myosin head were assumed to be 1 pN (12), the number of the myosin molecules involved in the bead movement would be only 1 to 20. On the other hand, the maximum velocity of the bead

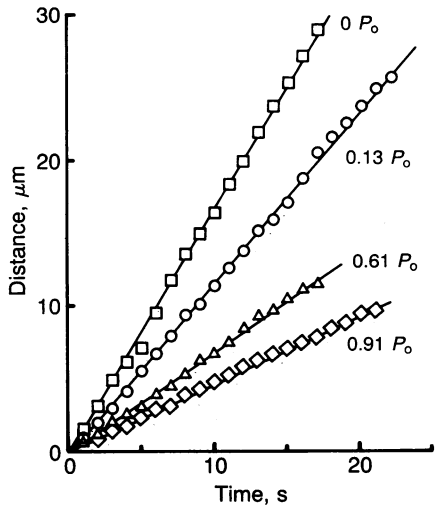

FIG. 3. Constant velocity movements of a myosin-coated bead on the actin cables under four different amounts of positive load. The amount of load on the bead is expressed relative to P_o. Regression lines were drawn by the least-squares method. The amount of P_o was 15 pN.

movement (V_{max}) in the unloaded condition showed a much smaller variation of 1.6–3.6 μm/s (mean 2.0 μm/s; n = 18).

In the microscopic observation and recording of bead movement, all of the beads observed were kept well in focus during their movement over a distance of >500 to ≈1,000 μm. As the beads could be made out of focus by moving the objective up or down by 2 μm, the actin cables on which the beads were moving were very closely in parallel with the rotor plane.

In agreement with the previous report (1), linear bead aggregates were frequently observed to move smoothly on the actin cables without changing their configuration. This may be taken to indicate that the bead movement may not be accompanied by its rotation. Another reason that makes the bead rotation unlikely is the large variation of P_o among the beads; since the variation of P_o may reflect a marked topographical variation in the number of myosin heads available for the bead movement, the constant velocity bead movement under positive loads may not take place over a long distance if the movement is associated with the bead rotation, resulting in a marked change in the number of myosin beads involved in the bead movement.

Steady-State Relation Between the Force and the Velocity of the Bead Movement in the Positive Load Region. The steady-state P–V relation of the bead movement was studied by applying various centrifugal forces opposite to the bead movement to serve as positive loads. The bead was allowed to move for 10–20 s under each centrifugal force applied. During the determination of the P–V relation, the magnitude of centrifugal force was either gradually increased or randomly altered with similar results. A typical example of the steady-state P–V relation obtained from the beads with high value of P_o (10–39 pN) is shown in Fig. 4. Similar results were obtained with nine other beads studied.

The P–V curve was fitted to a hyperbola (a/P_o = 0.4–0.8) in the low-force range from zero to 0.3–0.5 P_o. In the high-force range from 0.3–0.5 P_o to 1.0 P_o, on the other hand, the velocity decreased, with rates increasing with increasing forces until it reached zero at P_o. The velocity above which the P–V curve was hyperbolic in shape up to V_{max} was 0.3–0.4 V_{max}. The P–V curve obtained differs from the hyperbolic P–V relation of whole muscle (7), but it has been shown by Edman (8) that the P–V curve of single muscle fibers deviates from a hyperbola in the high-force range

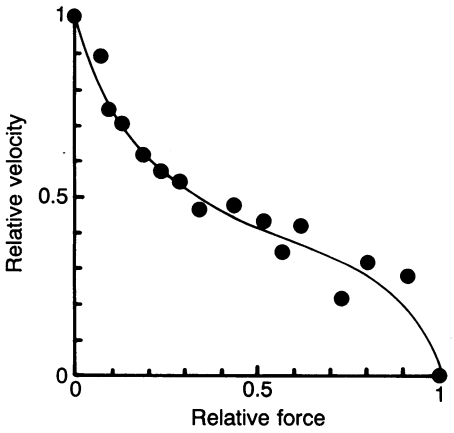

FIG. 4. Typical example of the steady-state *P–V* relations of the bead movement in the positive load region, obtained from the beads with high P_o values (10–39 pN). Data points were obtained in a random order. The velocity and the force (= load) values are expressed relatively to V_{max} and P_o, respectively. The curve in the low-force range (from 0 to 0.4 P_o in this case) was fitted to a hyperbola (a/P_o = 0.8) by the nonlinear least-squares method. The results shown in Figs. 3 and 4 were obtained from one and the same bead.

above 0.8 P_o, thus giving rise to a double hyperbolic *P–V* curve. Our present impression is that the *P–V* curve of the myosin-coated bead movement along the actin cables is analogous in shape to the double hyperbolic *P–V* curve of single muscle fibers, though a marked difference in the break point exists between them. These results may be taken to indicate that our *in vitro* assay system may retain the basic characteristics of contracting muscle fibers. No attempts were made to fit the *P–V* curve in the high force range to another hyperbola because of a large scatter of data points.

It was also possible to obtain the *P–V* relation on five beads with low values of P_o (3.5–5.9 pN). Fig. 5 shows an example. Compared with the *P–V* curve of the beads with high P_o (Fig. 4), the hyperbolic part of the *P–V* curve in the low-force range was much less pronounced, being confined to the velocity range above 0.6–0.8 V_{max}. It was not possible to study the *P–V* relation on the beads with P_o of 1–2 pN, partly because it was not easy to observe the bead movement at low rates of rotor rotation and partly because the beads tended not to move smoothly over a long distance.

Steady-State Relation Between the Force and the Velocity of the Bead Movement in the Negative Load Region. Since the

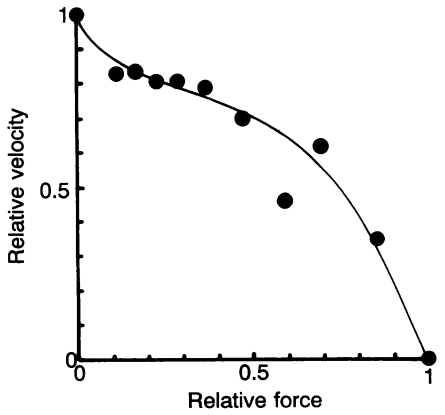

FIG. 5. Example of the steady-state *P–V* relations of the bead movement obtained from the beads with low P_o values (3.5–5.9 pN). The data points were obtained in a random order from a bead with P_o of 3.8 pN. Note the difference in shape between the curves shown in Figs. 4 and 5.

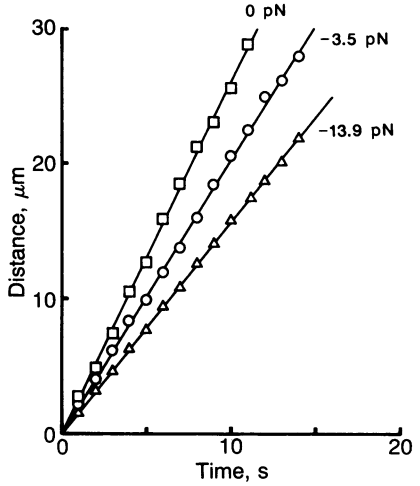

FIG. 6. Constant velocity movements of a myosin-coated bead on the actin cables under three different amounts of negative load. The amount of load on the bead is expressed in pN. Regression lines were drawn by the least-squares method. Note that the velocity of the bead movement decreases with decreasing amount of negative load.

polarity of the actin cable, which determines the direction of the bead movement, is reversed across the indifferent zone (1, 2), we also took the opportunity to apply centrifugal forces to the beads in a direction similar to the bead movement to serve as negative loads (Fig. 1*B*). As with positive loads, the beads moved with a constant velocity under a given negative load (Fig. 6). To our surprise, however, the velocity of the bead movement did not increase, though the beads were pushed by the applied centrifugal forces. In 15 of 18 beads studied, the velocity of the bead movement first decreased with increasing negative loads, reaching a minimum that was 20–60% lower than the initial unloaded velocity (V_{max}); with further increasing negative loads, the velocity increased toward the initial unloaded velocity until the bead was detached from the actin cables to flow away in the direction of the applied centrifugal force. Fig. 7 shows an example of the steady-state *P–V* relation in the negative load region. As with P_o, the force at which the bead was detached from the actin cables showed a wide variation ranging from 1.3 to 25 pN (mean, 7 pN; n = 12). Since it was not technically possible to apply both positive and negative loads to the same bead, the amount of the critical negative loads could not be expressed relative to P_o. The extent of decrease in the velocity

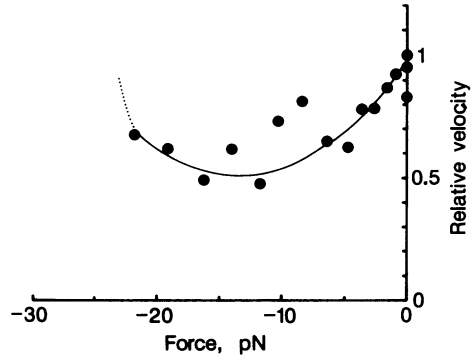

FIG. 7. Steady-state *P–V* relation of the bead movement in the negative-load region. Data points were obtained in a random order. The velocity values are expressed relative to V_{max}, while the force (= load) values are expressed in pN. The results shown in Figs. 6 and 7 were obtained from the same bead. The bead was detached from the actin cables with a negative load of ≈25 pN.

of the bead movement under negative loads was also variable, ranging from 20% to 60% of V_{max}.

With respect to the rest of the three beads studied, on the other hand, the velocity of the bead movement did not change appreciably under negative loads until the bead was detached from the actin cables. The shape of the steady-state *P–V* relation in the negative-load region (Fig. 7) remained unchanged when the amount of load was changed in a random order, though the velocity for a given amount of load tended to decrease with repeated application of the load.

Effect of Centrifugal Forces on the Rigor Actin–Myosin Linkages. When the ATP was removed from Mg·ATP solution, all the myosin-coated beads attached firmly to the actin cables because of the formation of rigor linkages between actin and myosin. These beads did not move at all, at least for 30–60 s, even with centrifugal forces producing both positive and negative loads up to 47 pN.

DISCUSSION

In this study, we have succeeded in obtaining the steady-state relation between the force and the sliding velocity of the actin–myosin interaction coupled with ATP hydrolysis, using the centrifuge microscope to apply constant centrifugal forces to the myosin-coated beads moving on the actin cables. Under a constant positive load, the beads moved on the actin cables with a constant velocity over many micrometers (Fig. 3). The steady bead movement is caused by the myosin molecules interacting with the actin cables, and the range of P_o measured (1.9–39 pN) indicates that the number of the myosin molecules involved in the bead movement may be very small, being only 1–20 (12). Thus, the present assay system provides a condition much simpler than that of the actin–myosin interaction taking place in contracting muscle; the distance of sliding between actin and myosin filaments in the physiological contraction is limited to ≈ 1 μm in each half sarcomere, and the filament sliding is always accompanied by an increase in the amount of overlap between the filaments. Even in a single muscle fiber with P_o of 10^{-3} N, the number of the actin–myosin linkages involved in the isometric force generation may be $\approx 10^9$ in each half sarcomere.

On this basis, it is of interest that the *P–V* curve analogous in shape to that in single muscle fibers is obtained from the beads with P_o of 3.5–39 pN (Figs. 4 and 5). As the bead movement is thought to be caused by 2–20 myosin molecules or 4–40 myosin heads, these results may be taken to imply that the observed *P–V* relation largely reflects the dynamic characteristic of individual myosin molecule or myosin head, though it has been widely held that the *P–V* curve in contracting muscle largely reflects the change in the number of myosin heads involved in the force generation and the myofilament sliding (13).

The most remarkable result brought about in the present study is that, under centrifugal forces serving as negative loads, the velocity of the bead movement mostly decreased by 20–60% from the initial unloaded velocity (V_{max}) until the beads were eventually detached from the actin cables (Figs. 6 and 7). It seems difficult to explain the above unexpected nature of the actin–myosin sliding in terms of the contraction model of Huxley (13) in which V_{max} is determined by a balance between positive and negative forces generated by the actin–myosin linkages in the unloaded condition.

In the present experiments, the centrifugal force vector can be considered as applied at the center of the bead, while the force generated by the myosin molecules is at the bead surface in contact with the actin cables. These forces might produce an appreciable torque on the bead, and the torque might either push the myosin head onto the actin cables or pull it apart from the cables, depending on the direction and the magnitude of centrifugal force. However, the myosin heads extend randomly from the myosin aggregate on the bead to interact with the actin cables. Thus, the contact between the bead and the actin cables differs from the contact between a solid sphere and a solid plane, suggesting that the torque on the bead may not be large enough to seriously affect the bead movement.

As far as we know, a possible mechanism of the actin–myosin sliding that can explain the decrease in the sliding velocity between actin and myosin by negative loads is the self-induced translation model of Mitsui and Ohshima (14) in which the attachment of the myosin head induces local conformational changes in the actin filament to generate an axial gradient of electrostatic force, causing the sliding of the myosin head along the actin filament. Though this does not necessarily mean that this contraction model is correct, such a mechanism should be seriously considered.

Using the slack test method, Edman (15) showed that the shortening velocity of a single muscle fiber can be increased above V_{max} if the resting force is present. It seems possible that, in his experiments, the actin–myosin linkages are inactivated by a quick release, so that the slackened fiber could be made taut quickly by the elastic restoring force other than the actin–myosin interaction.

Finally, we emphasize that the present force–movement assay system is very useful not only in eliminating the gap between muscle biochemistry and muscle physiology but also in revealing the unexpected features of the ATP-dependent actin–myosin sliding, which are difficult to observe by any other means.

This work was supported by the Science Research Promotion Fund from Japan Private School Promotion Foundation (to H.S.) and by Grant-in-Aid for Scientific Research 62300017 from the Ministry of Education, Science and Culture of Japan (to H.S.).

1. Sheetz, M. P. & Spudich, J. A. (1983) *Nature (London)* **303,** 31–35.
2. Shimmen, T. & Yano, M. (1984) *Protoplasma* **121,** 132–137.
3. Kron, S. J. & Spudich, J. A. (1986) *Proc. Natl. Acad. Sci. USA* **83,** 6272–6276.
4. Harada, Y., Noguchi, A., Kishino, A. & Yanagida, T. (1987) *Nature (London)* **326,** 805–808.
5. Chaen, S., Oiwa, K., Shimmen, T., Iwamoto, H. & Sugi, H. (1989) *Proc. Natl. Acad. Sci. USA* **86,** 1510–1514.
6. Iwamoto, H., Sugaya, R. & Sugi, H. (1990) *J. Physiol. (London)* **422,** 185–202.
7. Hill, A. V. (1938) *Proc. R. Soc. London Ser. B* **126,** 136–195.
8. Edman, K. A. P. (1988) *J. Physiol. (London)* **404,** 301–321.
9. Perry, S. V. (1955) *Methods Enzymol.* **2,** 582–588.
10. Tazawa, M., Kikuyama, M. & Shimmen, T. (1976) *Cell Struct. Funct.* **1,** 165–176.
11. Kamitsubo, E., Ohashi, Y. & Kikuyama, M. (1989) *Protoplasma* **152,** 148–155.
12. Hill, T. L. (1974) *Progr. Biophys. Mol. Biol.* **28,** 267–340.
13. Huxley, A. F. (1957) *Progr. Biophys. Biophys. Chem.* **7,** 257–318.
14. Mitsui, T. & Ohshima, H. (1988) *J. Muscle Res. Cell Motil.* **9,** 248–260.
15. Edman, K. A. P. (1979) *J. Physiol. (London)* **291,** 143–159.